Challenging Glass Conference Proceedings – Volume 10 – June 2026 – Louter, Bos & Belis (Eds.)
International Conference on the Architectural and Structural Application of Glass
Challenging Glass Conference 10 – 15-17 June 2026 – TU Delft – The Netherlands

Cyclic Out-of-Plane Bending Response of 2-ply Annealed Laminated Glass in the Partially Cracked Stage

Chiara Bedon [a], Nicola Cella [a], Luca Cozzarini [a]

a University of Trieste, Department of Engineering and Architecture, Italy
chiara.bedon@dia.units.it, nicola.cella@phd.units.it, lcozzarini@units.it

Abstract

The post-breakage security and structural safety analysis and quantification for laminated glass (LG) elements in constructions is a critical issue, and a rather challenging task, due to many influencing parameters and interconnected aspects that are hard to control and quantify. From a practical point of view, among many others, the glass type (and thus the associated size and shape of shards) is one of the most important influencing parameters for the residual capacity assessment in case of damage. The quantification of this residual capacity is carried out in this paper by introducing a sound estimation of the equivalent modulus of elasticity for cracked glass. To this aim, small-scale 2-ply LG specimens are investigated in a cyclic 3-point-bending (3PB) setup, with partial fracture corresponding to the "STAGE 2" of damage propagation for 2-ply LGs. A total of 57 tests is carried out, considering different parameters, such as the interlayer type and thickness, the glass thickness, the imposed deformation rate and amplitude. The comparative analysis of experimental results gives evidence of rather interesting mechanical performances in out-of-plane bending, which are certainly affected by the presence of a broken glass layer in STAGE 2, but still ensuring (even under a cyclic protocol) an interesting residual capacity for the damaged LG section.

Keywords

Glass, Laminated Glass, Partial Fracture, Damage, Experiments

Article Information

- Digital Object Identifier (DOI): 10.47982/cgc.10.768
- Published by Challenging Glass, on behalf of the author(s), at Stichting OpenAccess.
- Published as part of the peer-reviewed Challenging Glass Conference Proceedings, Volume 10, June 2026, 10.47982/cgc.10
- Editors: Christian Louter, Freek Bos & Jan Belis

1. Introduction

The post-breakage analysis of laminated glass (LG) is rather challenging, as it depends on many interconnected influencing parameters, and is strictly correlated to the structural safety of the element (Belis et al. 2026). According to design standards, it is expected that – in case of partial damage –the residual LG section can still provide a minimum mechanical capacity towards any possible sustained load (CNR-DT 201/2013; CEN TS 19100-2; CEN TS 19100-3). This poses a major uncertainty on the way to quantify and explicate the residual contribution of glass fragments.

So far, several studies proved that the type of glass (and thus the size and shape of fragments) is one of the most critical parameters: the larger is the size of fragments (i.e., as for annealed (AN) glass) and the smaller (and even negligible, according to design standards) is the expected effect in terms of residual out-of-plane bending stiffness. For the same reason, heat-strengthened (HS) and fully tempered (FT) glass types are often bonded together, to optimally combine tensile strength and post-breakage residual rigidity needs (CNR-DT 201/2013; CEN TS 19100-2; CEN TS 19100-3). Besides, there are many other aspects that should be taken into account (Bedon et al. 2025a; Xie et al. 2026), and the type of glass should be also correlated with the size of the sample (Zhou et al. 2025), or the fracture layout under loading (Bedon et al. 2025a), or the type of interlayer (Centelles et al. 2020), or the strain rate for interlock (Bedon et al. 2025b). In practical terms, the glass type alone can be hardly used to classify the mechanical performance of LG in the post-breakage stage.

This paper aligns with (Bedon et al. 2026) and poses the attention on the partially fractured, quasi-static cyclic response of small-scale 2-ply AN specimens, considering multiple aspects and configurations, for a total of 57 tests. The attention is given to the quantification of the equivalent modulus of elasticity of cracked glass ($E_{g,cr}$), which can well represent the mechanical contribution of glass fragments, compared to the nominal modulus of elasticity of intact glass E_g= 70 GPa (EN 572-8:2004). The study explores the so-called "STAGE 2" of Fig. 1, which is expected to offer mechanical performances that are comprised between the SM (single glass layer) and SI (intact LG) bounds.

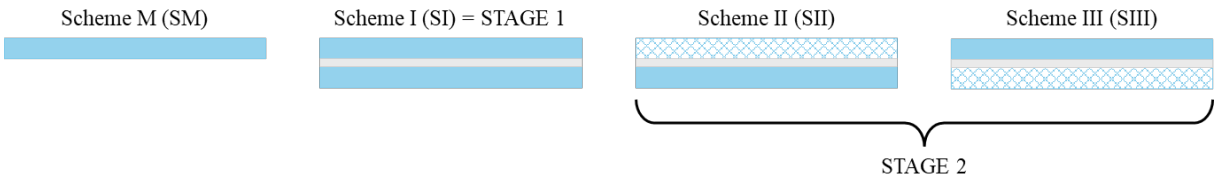

Fig. 1: Cross-sections of the considered configurations (pattern = broken layer).

A similar approach was used in (Bedon et al. 2025a), to quantify the residual capacity of LGs, where the analysis of 2-ply (8+8 mm) partially fractured AN glass specimens bonded by EVA film (500 mm × 1000 mm their size) resulted in $E_{g,cr}$= 69.9 GPa (ΔE= -0.14%) in SII and $E_{g,cr}$= 37.9 MPa (ΔE= -45.8%) in SIII. For small-scale LG samples, where the local effect of single cracks can be further magnified, literature experiments are reported in (Bedon and Santos 2023; Bedon and Fasan 2024) for AN plates with 40 mm × 100 mm size. The average $E_{g,cr}$ was calculated in 32.1 GPa (ΔE= -54.1%), which is rather in close agreement with SIII results recalled from (Bedon et al. 2025a). Most importantly, a progressive decrease in $E_{g,cr}$ was observed with increasing the number of imposed impacts, from an initial value of 53.4 GPa (ΔE= -23.7%), and down to 10.8 GPa (ΔE= -84.7%) after 20-25 imposed impacts. In the present experimental analysis, more in detail, $E_{g,cr}$ is derived from the average results of cyclic tests, to account for the possible effect of repeated loading steps.

2. Materials and methods

2.1. Specimens and cyclic bending experiments

The typical specimen consisted of a 2-ply LG section, composed of two AN glass plates and a bonding interlayer (Fig. 2). Each specimen measured 50 mm in width × 100 mm in length (Fig. 2 (a)). Variations through the experimental investigation included modification of the nominal glass thickness (t_g= 4 mm and 10 mm respectively), the interlayer thickness (t_{int}= 0.76 mm and 1.52 mm) and the type of interlayer (EVALAM VISUAL and SG5000 – labelled as "EVA" and "SG" in the following). These governing parameters were combined to reproduce different configurations, for a total of 57 tests. In doing so, one glass layer for each specimen was preliminary fractured by means of a steel hammer, to introduce in the experiments the effects of a partially fractured configuration (Fig. 2 (b)).

The typical 3-point-bending (3PB) test configuration is shown in Fig. 2 (a). During the execution of tests, both ends of LG plates were directly supported by steel blocks with rounded corners (5 mm the radius), placed 15 mm from the specimen ends. These blocks constrained the vertical displacement but allowed the rotation. Thus, the distance of supports for the 3PB test setup resulted in 70 mm.

Different test configurations were included in the experimental program. In particular, according to Fig. 1, the attention of the investigation in STAGE 2 was focused on the schemes SII (broken glass layer at the top) and SIII (broken glass layer at the bottom). The extended description of test methods is reported in (Bedon et al. 2026).

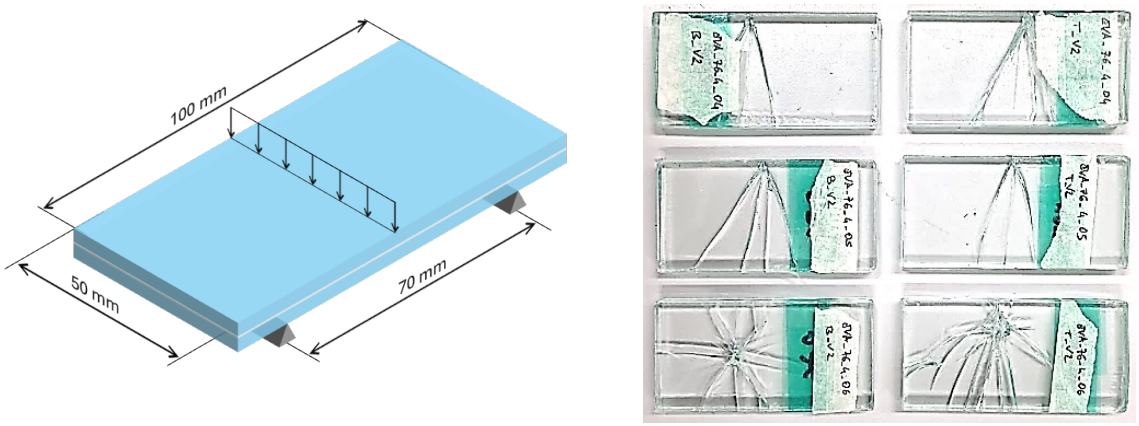

(a) (b)

Fig. 2: Quasi-static cyclic bending tests on partially fractured AN laminated glass specimens: (a) specimen size and setup and (b) examples of pre-cracked samples (top/bottom view).

Two different displacement rates, 25 mm/min (V1) and 250 mm/min (V2), were also used to explore the effect of loading rate, which is known to strongly affect the behaviour of the interlayers (Centelles et al. 2020; Chen et al. 2022; Elkilani et al. 2025).

All the LG specimens were subjected to 20 cycles of quasi-static imposed displacement (C01-C20), in order to address any possible degradation of mechanical parameters. To this aim, the attention was focused on the analysis of a force-displacement range that is still associated to a linear elastic response of the residual (still intact) glass layer, as it is expected to happen in STAGE 2. Due to the high uncertainty on the actual tensile strength of AN glass (compared to the nominal characteristic value $\sigma_{t,ck}$ = 45 MPa), and the present research needs, the 3PB protocol was defined according to Fig. 3. First, the theoretical failure load $F_{u,SM}$ and the corresponding deflection $f_{u,SM}$ for the residual glass layer

was analytically calculated (i.e., SM configuration). This $f_{u,SM}$ value was then multiplied by 0.5 and considered as the reference deflection amplitude to impose the C01-C20 cycles to the LG specimens.

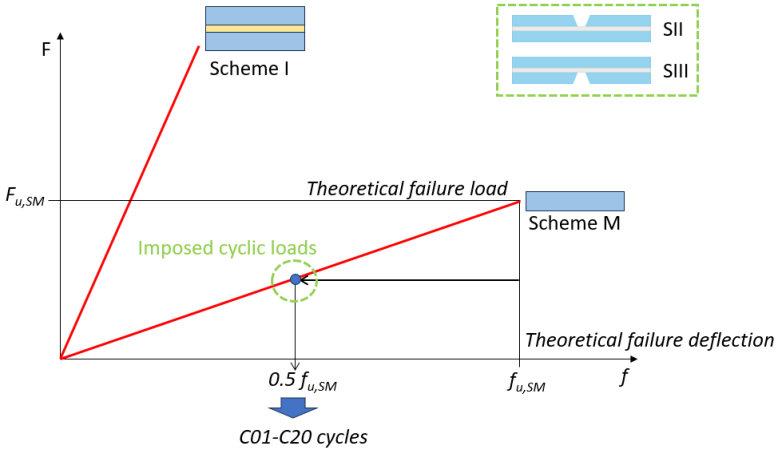

Fig. 3: Schematization of the approach for the definition of the imposed quasi-static cyclic protocol in the 3PB setup.

2.2. Equivalent modulus of elasticity for cracked glass

The Wölfel-Bennison analytical model (Wölfel 1987; CNR-DT 201/2013; ASTM E1300-09a) was adapted in this study to the typical setup of a 2-ply LG beam with a broken layer (Fig. 4). The original method, as known, quantifies the equivalent flexural stiffness EI_{eq} of a given 2-ply LG beam-like member, and implicitly accounts for the coupled response of the bonded components.

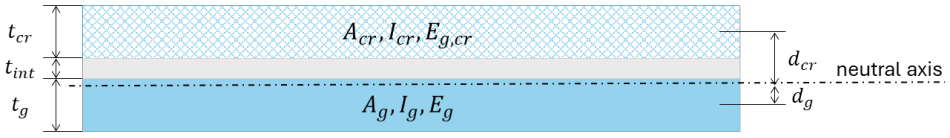

Fig. 4: Reference geometrical parameters for the calculation of $E_{g,cr}$.

In particular, the moment of inertia can be expressed as:

$$I_{eq} = I_g + n_E I_{cr} + \Gamma A^* d^2 \tag{1}$$

with:

$$n_E = \frac{E_{g,cr}}{E_g} \tag{2}$$

$$A^* = \frac{A_g \cdot n_E A_{cr}}{A_g + n A_{cr}} \tag{3}$$

$$d = d_g + d_{cr} \tag{4}$$

$$\Gamma = \frac{1}{1 + 9.6 \frac{t_{int} E_g I_s}{G_{int} L^2 d^2}} \tag{5}$$

$$I_s = t_g d_g^2 + t_{cr} d_{cr}^2 \tag{6}$$

Once the input G_{int} values are known for the examined configuration (2.68 MPa for EVA and 67.11 MPa for SG, respectively (Bedon et al. 2026)), the equivalent cracked modulus of the broken layer can be calculated as:

$$E_{g,cr} = \frac{E_g\left(I_{eq} - I_g - \Gamma A^* d^2\right)}{I_{cr}} \tag{7}$$

It is important to note that the equivalent cracked modulus is closely linked not only to the LG configuration under consideration, but also to the boundary conditions of the LG member, including mechanical restraints, load type and temperature. In this case, the simplified coefficient 9.6 was used in Eq. (5) following the general proposal of the Wölfel-Bennison. Whilst it is known that it can be hardly applied to different loading and boundary conditions, it is still accurate for the deflection analysis of simply supported LG beams under mid-span concentrated loads, as also reported in (Calderone et al. 2009). Very small scatter for the deflection analysis of the same configuration has been also reported in (Galuppi et al. 2013).

3. Results

3.1. Experimental observations

In the analysis of test results, a primary role was assigned to vertical displacement acquisitions during the 3PB tests. In addition to traditional machine records, Digital Image Correlation (DIC) techniques were also used (Fig. 5). Compared to the SI layout, as expected, the presence of a fractured glass layer led to a marked reduction of bending stiffness, which was properly captured by deflection analysis. Interestingly, the number of imposed cycles had a minor effect, and suggests a certain stability in the post-fracture performance for the tested LGs; see Fig 5(b). During the imposed cyclic protocol, the number of cracks was in fact typically observed to increase (see for example Fig. 6). On the other side, the bending stiffness of the composite section did not decrease proportionally. Moreover, no significant debonding was visually detected in the region of cracks.

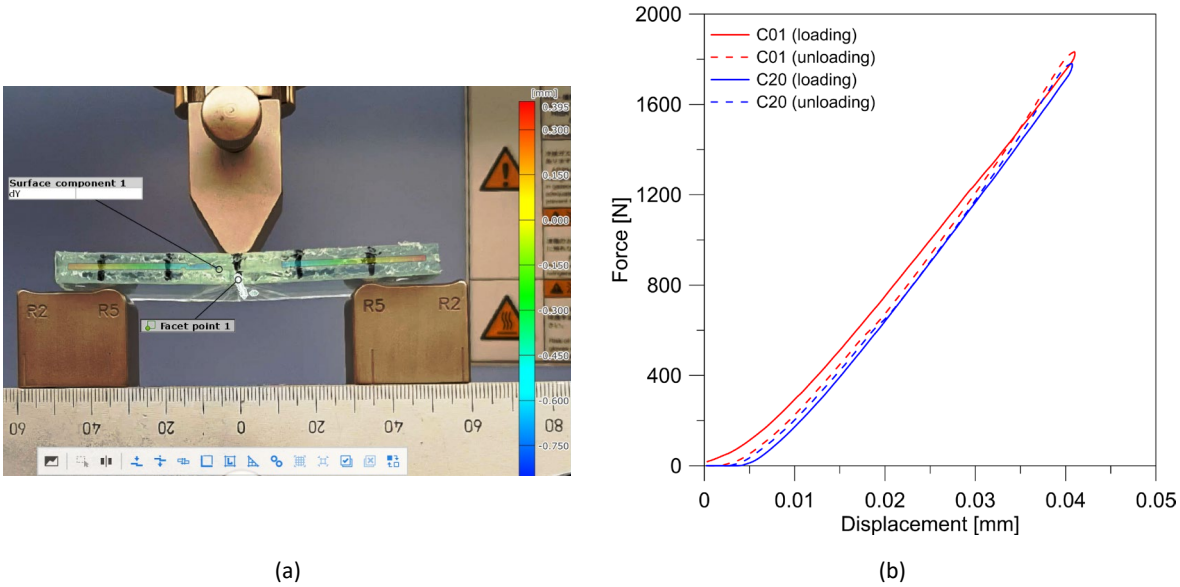

(a) (b)

Fig. 5: Experimental results: (a) DIC analysis during a 3PB test (deflection legend in mm) and (b) example of force-displacement curves.

(a) (b)

Fig. 6: Example of LG specimen: (a) with the preliminarily imposed crack and (b) after the cyclic protocol (bottom view).

3.2. Contribution of cracked glass

More relevant findings were observed by calculating the residual rigidity of the cracked glass layer, for each AN sample. In this regard, the mean and standard deviations values in Table 1 are calculated based on the n samples for each configuration and all cycles (C01-C20). At the same time, ΔE expresses the percentage variation with respect to the elastic modulus of intact glass (E_g = 70 GPa) as:

$$\Delta E = \frac{E_{g,cr} - E_g}{E_g} \tag{8}$$

In particular, the analysis of Table 1 suggests that the thickness of glass has a key role in the possible interlock of fragments. Considering both SII and SIII configurations, as well as EVA or SG interlayers, the V1 specimens with t_g= 10 mm can still offer a stiffness contribution. This effect is less pronounced for t_g= 4 mm. A similar trend can also be seen for both 10 mm and 4 mm thick glass layers when subjected to V2, both in SII and SIII.

For results in SII, it could be rationally expected that the increase in the equivalent modulus of elasticity with the glass thickness is related to the contact mechanism between the fragments on the compressive side of the specimen. As the thickness of the glass layer increases, the arm of the internal forces increases, and thus the overall stiffness. For results in SIII, the increase in stiffness is likely due to a tension stiffening mechanism of the interlayer, which is more pronounced with a thicker glass layer. Interestingly, the SG-bonded specimens in SII show an opposite trend with the glass thickness. This variation may be due to either the type of interlayer or to the random fracture pattern. Further tests are needed to investigate this phenomenon in detail. In any case, for most of the reported configurations $E_{g,cr}$ is always higher than zero (as in the typical design assumption recommended by standards).

Table 1: Calculated equivalent modulus of elasticity for the cracked glass layer ($E_{g,cr}$) in SII and SIII configurations (average value from series of n° samples).

					V1			V2	
		t_{int} [mm]	t_g [mm]	n°	$E_{g,cr}$ (± st.dev.) [GPa]	ΔE [%]	n°	$E_{g,cr}$ (± st.dev.) [GPa]	ΔE [%]
EVA	SII	1.52	10	2	16.6 ± 1.14	-76.3			
			4	1	5.31 ± 0.13	-92.4			
		0.76	10	2	23.65 ± 5.38	-66.2	3	25.27 ± 15.16	-77.4
			4	2	7.62 ± 1.28	-89.1	3	11.16 ± 2.88	-84.1
	SIII	1.52	10	4	14.08 ± 15.04	-79.9			
			4	1	0.13 ± 0.11	-99.8			
		0.76	10	3	31.69 ± 6.68	-54.7	3	35.98 ± 9.16	-71.0
			4	2	2.73 ± 1.22	-96.1	3	7.88 ± 2.06	-99.9
SG	SII	1.52	10	3	13.31 ± 4.61	-81.0			
			4	2	17.48 ± 0.88	-75.0			
		0.76	10	3	22.6 ± 8.31	-67.7			
			4	3	22.75 ± 3.16	-67.5			
	SIII	1.52	10	3	18.46 ± 6.56	-73.6			
			4	2	8.72 ± 4.36	-87.5			
		0.76	10	4	15.57 ± 3.31	-77.8			
			4	2	11.26 ± 1.25	-83.9			

Trying to compare the present and past experimental results, a direct correlation is indeed hard to generalize, and further studies are required. Considering for example the short-term/small-amplitude loads applied in (Bedon et al. 2025a) to large-scale EVA-bonded 2-ply AN samples, some preliminary considerations can be drawn (Table 2). In particular, the single crack effect is directly correlated to the size of the LG specimen.

Table 2: Qualitative comparison of present and literature results, in terms of calculated (average) equivalent modulus of elasticity for the cracked glass layer ($E_{g,cr}$) in SII and SIII configurations, based on different experimental investigations (all samples with EVA interlayer).

		Small-scale specimen (present study) [20 cycles]			Large-scale specimen (Bedon et al., 2025a) [Single loading step]		
Size		50 mm × 100 mm			500 mm × 1000 mm		
Imposed deflection/span ratio		≈ 1/1750 in SII and SIII			≈1/23000 in SII ≈1/10600 in SIII		
	t_{int} [mm]	t_g [mm]	$E_{g,cr}$ [GPa]	ΔE [%]	t_g [mm]	$E_{g,cr}$ [GPa]	ΔE [%]
SII	0.76	10	23.65	-66.2	8	69.9	-0.14
		4	7.62	-89.1			
SIII	0.76	10	31.69	-54.7	8	37.9	-45.8
		4	2.73	-96.1			

3.3. Further considerations

In practical terms, it is clear that the relevance of any possible residual capacity for partially cracked LGs is of utmost importance for structural safety and design optimization. To further highlight these evidences, parametric analytical calculations are carried out for the LG specimens in out-of-plane bending described in Section 2.1 (t_g= 4 mm and t_{int}= 0.76 mm, with 100 N the imposed mid-span load). In Fig. 7, the sensitivity of the LG package to the possible contribution of fragments is shown in terms of calculated mid-span deflection (Fig. 7 (a)) and maximum stress in the intact glass layer (Fig. 7 (b)), as a function of the equivalent modulus of elasticity for cracked glass, which ideally varies between 0 GPa (Scheme M) and 70 GPa (Scheme I). At the same time, different values of shear transfer coefficient Γ are also accounted between 0 (weak bond) and 1 (ideally rigid bond), for investigating the additional influence of the degree of shear coupling offered by the interlayer.

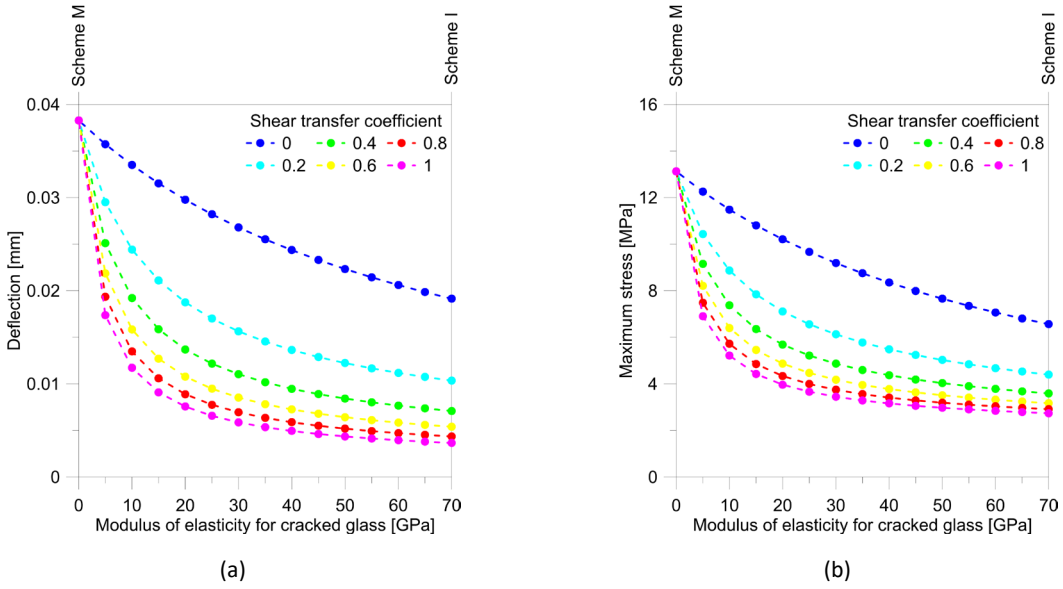

Fig. 7: Variation of (a) deflection and (b) maximum stress in the intact glass layer of a 2-ply LG element, as a function of equivalent modulus for cracked glass layer, for different shear transfer coefficient values.

As expected, the reduction of the modulus of elasticity for the cracked glass layer leads to a marked increase in the calculated deflection, as well as in the corresponding maximum stress in the intact glass layer. Compared to the approach recommended by technical guidelines (i.e., CNR-DT 201/2013), which conservatively prescribe to completely disregard the broken layer (Scheme M), the inclusion of the cracked layer with a reduced equivalent modulus is associated to a marked decrease of the predicted stress and deflection values in the residual cross-section, leading to an optimized design of LG sections. Notably, the variation of stress and deflection estimates is more pronounced for higher values of shear transfer coefficient (stiff interlayer).

This aspect is also highlighted in Fig. 8 in terms of deflection and stress ratio, where the modular ratio compares the equivalent cracked value to the intact one. It is worth noting that the variation for different shear transfer coefficients is negligible for modular ratios higher than 0.5. In practical terms, these analytical results indicate that an LG structural element consisting of a rigid interlayer and tempered glass layers, which in case of breakage are characterised by small fragments with a limited mechanical contribution to the overall flexural stiffness of the LG system (i.e., a small equivalent modulus of elasticity for the cracked glass layer), would be affected by a greater increase in stress in the still intact glass layer. Indeed, it can be seen that considering even a minimal mechanical contribution from broken glass could greatly reduce the maximum stress in the intact layer, compared to Scheme M.

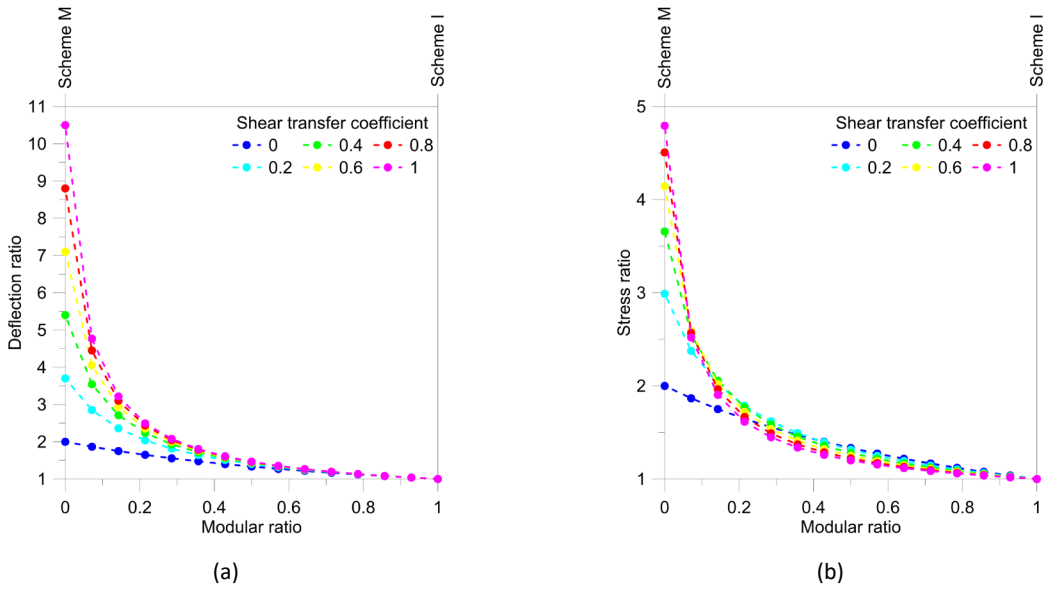

Fig. 8: Normalized comparison of (a) deflection and (b) stress ratio for a 2-ply LG element, as a function of modular ratio and for different shear transfer coefficient values.

4. Conclusions

In this paper, the attention is given to the experimental testing of partially fractured, laminated glass (LG) specimens composed of two layers of annealed glass. 57 different configurations in terms of glass thickness, interlayer type and thickness, displacement rate and artificial ageing were tested in a traditional three point bending setup.

The obtained results indicate that the flexural response of the cracked samples, despite being negatively affected by the presence of a cracked layer, maintains a notable residual mechanical capacity, even under cyclic loading. This evidence suggests that, based on the position of the broken layer, there is a phenomenon of interlocking of glass fragments and/or local stiffening of the interlayer that increases the bending stiffness of the LG package compared to the response of a single monolithic glass layer. The results presented here establish the foundations for further studies that will investigate the effect of additional parameters on the flexural response of partially cracked laminated glass.

Acknowledgements

These research activities are financially supported by the Italian Ministry of University and Research (MUR), via the FIS2021 Starting Grant (FIS00000609), www.hopglaz.it. Mr. Riccardo Del Bello is acknowledged for the technical support during the experimental investigation.

References

ASTM E1300-09a, Standard Practice for Determining Load Resistance of Glass in Buildings, American Society for Testing Material (ASTM), 2009

Bedon, C., Santos, F.A.: Effects of post-fracture repeated impacts and short-term temperature gradients on monolithic glass elements bonded by safety films. Composite Structures 319, 117166 (2023), https://doi.org/10.1016/j.compstruct.2023.117166

Bedon, C., Fasan, M.; Post-fracture stiffness and residual capacity assessment of film-retrofitted monolithic glass elements by frequency change, Math. Probl. Eng. 2024, 8922303 (2024), https://doi.org/10.1155/2024/8922303

Bedon, C., Kozlowski, M., Cella, N.: Gaps in the post-breakage out-of-plane bending stiffness assessment of 2-ply partially damaged laminated glass elements under short-term quasi-static loads, Eng. Struct. 327, 119617 (2025a), https://doi.org/10.1016/j.engstruct.2025.119617

Bedon, C., Cella, N., Del Bello, R.: Damage Assessment of Through-Cracked-Bending Laminated Glass Elements Under Low-Velocity Hard-Body Impacts, Materials 18(19), 4454 (2025b), https://doi.org/10.3390/ma18194454

Bedon, C., Del Bello, R., Cella, N., Cozzarini, L., Fasan, M.: Residual mechanical capacity of small-scale partially fractured annealed laminated glass elements subjected to a quasi-static cyclic protocol, Eng. Fail. Anal. 186, 110462 (2026), https://doi.org/10.1016/j.engfailanal.2025.110462

Belis, J., Kuntsche, J., Louter, C., Nielsen, J.H., Overend, M., Schneider, F., Schneider, J., Schula, S.: Engineering Glass Structures. Springer Nature Switzerland AG (2026), https://doi.org/10.1007/978-3-032-03233-1

Calderone, I., Davies, P.S., Bennison, S.J.: Effective laminate thickness for the design of laminated glass, in: Proceedings of Glass Performance Days 2009 (2009)

CEN TS 19100-2: Design of glass structures—Part 2: design of out-of-plane loaded glass components (Draft). European Committee for Standardization, Bruxelles, Belgium (2021)

CEN TS 19100-3: Design of glass structures—Part 3: design of in-plane loaded glass components and their mechanical joints (Draft). European Committee for Standardization, Bruxelles, Belgium (2021)

Centelles, X., Martín, M., Solé, A., Castro, J.R., Cabeza, L.F.: Tensile test on interlayer materials for laminated glass under diverse ageing conditions and strain rates, Constr. Build. Mater. 243, 118230 (2020), https://doi.org/10.1016/j.conbuildmat.2020.118230

Chen, S., Chen, Z., Chen, X., Schneider, J.: Evaluation of the delamination performance of polyvinyl-butyral laminated glass by through-cracked tensile tests, Constr. Build. Mater. 341, 127914 (2022), https://doi.org/10.1016/j.conbuildmat.2022.127914

CNR-DT 210/2013. Guide for the Design, Construction and Control of Buildings with Structural Glass Elements Consiglio Nazionale delle Ricerche (CNR), 2013

Elkilani, A., Elsisi, A., Elemem, H., Elbelbisi, A., Helal, Z., Salim, H.: Interlaminar bond strength of laminated glass composites under accelerated environmental effects, Construct. Build. Mater. 487, 142005 (2025), https://doi.org/10.1016/j.conbuildmat.2025.142005

EN 572-8:2004. Glass in building - Basic soda lime silicate glass products - Part 8: Supplied and final cut sizes. CEN, Brussels, Belgium, 2004

Galuppi, L., Manara, G., Royer-Carfagni, G.: Practical expressions for the design of laminated glass, Comp. Part B: Eng. 45(1), 1677-1688 (2013), https://doi.org/10.1016/j.compositesb.2012.09.073

Xie, D., Yang, J., Wang, X.-E., Wang, Y., Pan, Z., Zhao, C.: Temperature and time dependences of fragment generation and out-of-plane deformation in fractured tempered glass laminates. Thin. Wall. Struct. 218, 113959 (2026), https://doi.org/10.1016/j.tws.2025.113959

Wölfel, E.: Elastic composite: an approximation solution and its application possibilities, Stahlbau 6, 173-180 (1987).

Zhou, S., Biolzi, L., Simoncelli, M., Cattaneo, S.: Scaling Effects on Post-failure Responses of Laminated Glass Plates under Uniform Pressure, Glass Performance Days (GPD) 2025, https://gpd.fi/wp-content/uploads/2025/05/GPD2025_ID253_Zhou-et-al.pdf

Challenging Glass Conference Proceedings – Volume 10 – June 2026 – Louter, Bos & Belis (Eds.)
International Conference on the Architectural and Structural Application of Glass
Challenging Glass Conference 10 – 15-17 June 2026 – TU Delft – The Netherlands

Platinum Sponsor

SAINT-GOBAIN

Gold Sponsors

EASTMAN

kuraray

NorthGlass®

sedak

seele

Silver Sponsors

DOW®

octatube

PERMASTEELISA GROUP

SEEN

Organisation

TU Delft

Technische Universität München

GHENT UNIVERSITY